Exposure and Health
https://doi.org/10.1007/s12403-023-00572-x

ORIGINAL PAPER

Long-Term Atmosphere Surveillance (2016–2021) of $PM_{2.5}$-bound Polycyclic Aromatic Hydrocarbons and Health Risk Assessment in Yangtze River Delta, China

Keqin Wu[1,2] · Yuyang Yao[1] · Yuanhua Meng[1,2] · Xuhui Zhang[1] · Run Zhou[1,2] · Wenwei Liu[1,2] · Xinliang Ding[1,2]

Received: 20 October 2022 / Revised: 6 April 2023 / Accepted: 17 May 2023

Abstract
Long-term atmospheric quality monitoring of fine particulate matter ($PM_{2.5}$) and $PM_{2.5}$-bound polycyclic aromatic hydrocarbons (PAHs) was performed in Wuxi from 2016 to 2021. In total, 504 atmospheric $PM_{2.5}$ samples were collected, and $PM_{2.5}$-bound 16 PAHs were detected. The $PM_{2.5}$ and ∑PAHs level decreased annually from 2016 to 2021, from 64.3 to 34.0 μg/m^3 and 5.27 to 4.22 ng/m^3, respectively. The benzo[a]pyrene (BaP) levels of 42% of the monitoring days in 2017 exceeded the recommended European Union (EU) health-based standard of 1 ng/m^3. Five- and six-ring PAHs were found, including benz[a]anthracene, benzo[k]fluoranthene (Bkf), BaP, and benzo[g,h,i]perylene, which were the dominant components (indicating a prominent petroleum, biomass, and coal combustion contribution) using molecular diagnostic ratios and positive matrix factorization analysis. Moreover, $PM_{2.5}$ and PAHs were significantly negatively associated with local precipitation over a period of six years. Statistically significant temporal and spatial distribution differences of $PM_{2.5}$, and ∑PAHs were also found. The toxicity equivalent quotient (TEQ) of total PAHs was 0.70, and the TEQ of BaP (0.178) was the highest, followed by that of Bkf (0.090), dibenz[a,h]anthracene (Dah) (0.048), and indeno[1,2,3-cd]pyrene (0.034). The medians of the incremental lifetime cancer risk for long-term exposure to PAHs were 2.74E−8, 1.98E−8, and 1.71E−7 for children, teenagers, and adults, respectively, indicating that the carcinogenic risk of PAHs pollution in air was acceptable to local residents in this area. Sensitivity analysis revealed that BaP, Bkf, and Dah significantly contributed to carcinogenic toxicity. This research provides comprehensive statistics on the local air persistent organic pollutants profile, helps to identify the principal pollution source and compounds, and contributes to the prevention of regional air pollution.

Keqin Wu and Yuyang Yao contribute equally to this study and should be regarded as joint first authors.

✉ Xinliang Ding
dingxinliang@njmu.edu.cn

[1] Wuxi Center for Disease Control and Prevention (The Affiliated Wuxi Center for Disease Control and Prevention, Nanjing Medical University), Wuxi 214023, China

[2] Research Base for Environment and Health in Wuxi, Chinese Center for Disease Control and Prevention, Wuxi 214023, China

Published online: 24 May 2023

Graphical Abstract

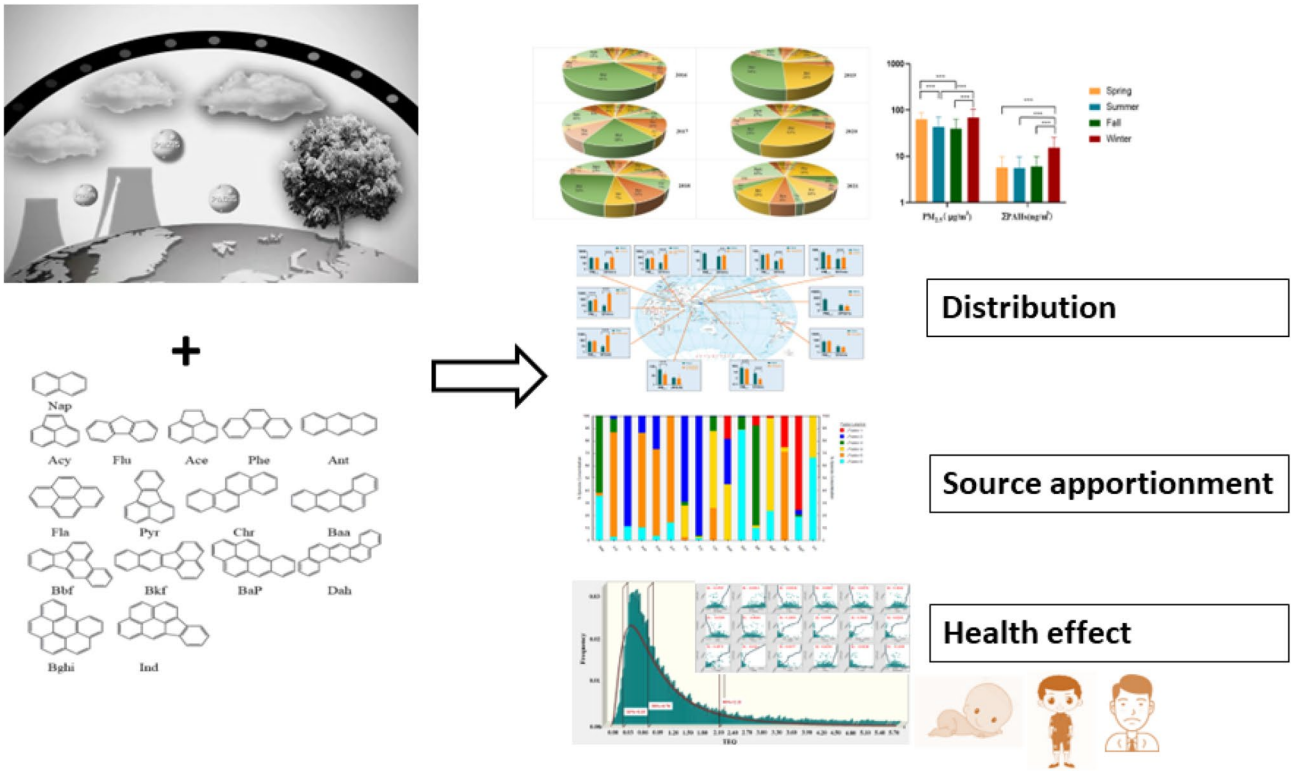

Keywords $PM_{2.5}$ · PAH · Spatial distribution · Risk assessment · Monte Carlo · Source apportionment

Introduction

Air pollution causes millions of deaths annually and is attributed to multiple adverse birth outcomes, such as obesity, lung malfunction, and asthma (Hsu et al. 2020; Toriba and Hayakawa 2021). The Global Burden of Diseases in 2019 indicated that particulate matter pollution was the second-leading level 3 risk factor for disability-adjusted life years (DALYs) among all risks. In 2019, it caused approximately 210 million DALYs and 6.45 million deaths worldwide. Statistics show that deaths resulting from outdoor air pollution are conservatively estimated at between 350,000 and 500,000 in China annually. The economic losses caused by related health costs have accounted for 1.16–3.8% of the gross domestic product (Ma et al. 2021). A 1% increase in population density causes a 0.214% increase in daily fine particulate matter ($PM_{2.5}$); however, industrialization, energy consumption, and traffic pollution also significantly increase the $PM_{2.5}$ accumulation rate (Lou et al. 2016).

Polycyclic aromatic hydrocarbons (PAHs), such as benzo[a]pyrene (BaP), comprise two or more fused aromatic rings arranged in various configurations (Nagato 2018). PAHs are released into the environment from natural and anthropogenic sources (WHO 2003). Anthropogenic activities, such as automobile exhaust emissions and industrial emissions, are reportedly the main sources of emissions (Yang et al. 2019; Fang et al. 2020). Epidemiological studies have found that workers exposed to multiple PAHs have a higher chance of developing skin, lung, bladder, and gastrointestinal cancers (Diggs et al. 2011). Similar outcomes have been observed in laboratory animal experiments (Le Goff et al. 2019; Yazdani 2020). PAHs carcinogens, including benzo[a]anthracene (Baa), BaP, and dibenz[ah]anthracene (Dah), have been identified (U.S. EPA 2017; Idowu et al. 2019). Based on their toxicity to humans, the U.S. Environmental Protection Agency (EPA) has designated 16 priority PAHs, which have been continuously monitored worldwide for decades (Andersson and Achten 2015). $PM_{2.5}$-bound PAHs formed through incomplete combustion of organic materials are the primary organic components in $PM_{2.5}$. PAHs are widely distributed in the air and can be carried over long distances (Ravindra et al. 2008). Moreover, PAHs combined with $PM_{2.5}$, can persistently exist in the environment longer than those in the unbound state (Stanišić et al. 2021). Therefore, PAH exposure is closely correlated to the condition of $PM_{2.5}$, particularly in winter when PAH levels

could increase with the change in air temperature, reduction in photolysis, decomposition of radicals, and decreases in particle deposition (Rezaei et al. 2018). $PM_{2.5}$-bound PAHs can penetrate lungs deeply and even enter the bloodstream, causing cardiorespiratory diseases, which have been found in brick-kiln workers and chronic obstructive pulmonary disease (COPD) patients (Berumen-Rodríguez et al. 2021; Che et al. 2020). PAHs were among the first atmospheric pollutants to be designated as suspected carcinogens (Kim et al. 2013). The European Union (EU) has established a health-based standard for PAHs, with the concentration of target PAHs, BaP in ambient air limited to 1 ng/m^3 (European Commission 2019). China has also formulated a standard of toxic equivalent quotient (TEQ) for BaP, and the BaP-TEQ must be controlled at less than 2.5 ng/m^3 for daily and 1.0 ng/m^3 for annual average. However, current researches have revealed that the BaP-TEQ in several urban cities in China and other countries were higher than the prescribed limits (Fan et al. 2019; Kang et al. 2020; Yu et al. 2022).

As one of the most developed areas, the Yangtze River Delta region plays an essential role in the economic development of China. Moreover, with the rapid expansion of industrialization and urbanization, numerous issues associated with the carrying capacity of resources, environment and population have recently emerged (Zhao et al. 2020). The rising energy consumption and remarkable increase in private cars have caused more severe pollution in this region than in other cities (Wang et al. 2017; Mao et al. 2020). Wuxi is located in the south of Jiangsu Province, in the middle of the Yangtze River Delta, with an area of 4650 km^2 and a population of 7.46 million as of 2021. Studies have reported that the air quality in Wuxi is worse than that in other cities such as Ningbo and Shaoxing (Yu et al. 2020). However, most previous studies have concentrated on particulate matter with aerodynamic diameters of < 2.5 and < 10 μm, sulfur dioxide (SO_2), nitrogen dioxide (NO_2), and several metals (Zhu et al. 2017; Chen et al. 2020; Wang et al. 2020).

In this study, we conducted long-term monitoring of $PM_{2.5}$-bound 16 PAHs, recommended by the US EPA in Wuxi for six consecutive years from 2016 to 2021. The temporal distribution characteristics, including seasonal variations, compositions, annual trends, and source appointments, which were analyzed by molecular diagnostic ratio (MDR) and positive matrix factorization (PMF), were comprehensively described. Moreover, spatial distribution characteristics of this study were compared with those of existing studies. Subsequently, dynamic 10,000 simulations of the toxicity assessment and incremental lifetime cancer risk (ILCR) were then performed using Crystal Ball. Sensitivity analysis was also performed to further understand the risk factors. Through long-term surveillance, our study can provide detailed statistics on the adverse health effects of $PM_{2.5}$-bound PAHs on local humans, help identify potential pollution sources, and promote optimal regional air quality.

Materials and Methods

Sample Collection

The $PM_{2.5}$ sampling site was set in the Binhu District, the central urban area within the state-controlled environmental air quality monitoring station coverage in Wuxi (31°07′ to 32°02′, 119°31′ to 120°36′), as shown in Fig. 1. The distance between the sampling site and the main traffic road is approximately 30 m. There is no pollution source such a chemical or processing plant nearby. The nearest hospital is approximately 600 m away, and the nearest gas station is approximately 900 m away. Detailed sampling methods have been described in our previous study (Wu et al. 2022). A ZR3920 intelligent medium-flow ambient air particulate matter sampler (Qingdao Zhongrui, China) equipped with a 90-mm glass fiber filter membrane (Waterman, UK) was used to collect the air samples. Before and after sampling, the filter membrane was equilibrated for 24 h in a constant temperature and humidity box before being weighed. The sampling flow rate was 100L/min, and the sampling volume was set to 120m^3. After collection, glass fiber filters were stored in a plastic filter box. The temperature, humidity, and air pressure were recorded to calculate the volume under standard conditions. The sampling period for each sample was 20 h per day. The seven samples were collected from the10th to the 16th of each month since January, 2016 to December, 2021. One field sample to be used for blank correction, was collected without the filter film connected to the sampler, and was analyzed using the same analysis procedure as the samples.

Chemicals and Reagents

Analytical standards for EPA priority 16 PAHs were purchased from Sigma-Aldrich Inc. (North Charleston, SC, USA). The structures and details of the 16 PAHs are shown in Fig. S1. Chromatography-grade acetonitrile and methanol were purchased from Merck (New Jersey, USA). Deionized water was purified using the ELGA Purelab Ultra system (Vivendi Water Systems, Buckinghamshire, UK).

Analyses of PAHs

A quarter of the sample filter film was cut into pieces with ceramic scissors, and 4.5 mL acetonitrile was added into a 15 mL centrifuge tube. Ultrasonography was performed at 35 °C for 30 min, following which the supernatant was removed and cooled to room temperature (approximately at

Fig. 1 $PM_{2.5}$ sampling site in Wuxi city

25 °C). The filtrate was filtered through a 0.45 μm microporous membrane and subjected to sampling liquid chromatographic determination. A liquid chromatograph with a diode array tandem fluorescence detector (Agilent Technologies Inc., Santa Clara, CA, USA) was used for PAH determination. The chromatographic column was a CNW Athena PAHs C18 column (250 mm × 4.6 mm, 5 μm, Shanghai Ampo Experimental Technology). The injection volume was 20μL. Details of the instrument parameter settings can be found in our previous study (Yao et al. 2021). The results of the PAH analysis are summarized in Table S1. The same methodology and technical personnel were employed for all observations during the entire study period to maintain consistency and accuracy of data. Quality control samples were added by inserting low, medium and high levels of a standard mixture per 10 samples and the variation was less than 10%.

Source Apportionment

MDRs have been used for PAHs source identification for decades. The MDRs are based on the assumption that each PAH emitting source releases PAH at the same ratio and are calculated using the ratios of specific pair-PAHs. PMF is a frequently used receptor model for multivariate factor analysis (Paatero and Tapper 1994; Paatero 1997). The U.S. EPA PMF5.0 was used to conduct source apportionment. The details of PMF overview and operation can be found in the Fundamentals and User Guide (https://www.epa.gov). In total, five factors were applied and the percentages of each PAH contributing to the factors were calculated to find the feature components of each factor.

Health Risk Assessment

The US EPA describes human health risk assessment in four steps: hazard identification, exposure assessment, toxicity assessment, and risk characterization. The PAH exposure assessment was calculated using TEQ, which is the sum of the estimated cancer risk of all PAHs relative to BaP. The TEQ can be calculated using the following equation:

$$TEQ = \sum C_i \times TEF_i \quad (1)$$

Ci is the concentration of PAH and TEF_i is the toxicity equivalency factor. The value of TEF is 1 for BaP and Dah; 0.1 for Baa, Bkf, and Ind; 0.01 for Chr, Ant, and Bghi; and 0.001 for Nap, Acy, Ace, Flu, Phe, Fla, and Pyr (Nisbet and LaGoy 1992; Froehner et al. 2010).

The carcinogenic value is quantitatively represented by the ILCR using the following equation:

$$ILCR = \frac{CSF \times TEQ \times IR \times EF \times ED \times CF}{BW \times AT} \quad (2)$$

CSF is the inhalation cancer slope factor of BaP with a value of 3.14 per $mg \cdot kg^{-1} \cdot day^{-1}$, IR is the inhalation rate ($m^3 \cdot day^{-1}$), EF is the exposure frequency ($days \cdot year^{-1}$), ED is the exposure duration (years), CF is the conversion factor with a value of 10^{-6}, BW is the body weight (kg), and AT is the average lifespan of carcinogens (25,550 days). The population was divided into three groups by age: children (4–10 years), teenagers (11–17 years), and adults (18–70 years). The parameters for each group are listed in Table S2 (Yan et al. 2019).

Crystal ball 7.3 (Informer Technologies Inc., Los Angeles, CA USA) was used to conduct Monte Carlo simulations of forecast and risk analysis. For uncertain variables, such as concentration of PAHs or body weight, the simulations calculate numerous scenarios of a model by repeatedly picking values from the probability distribution. The Spider chart describes sensitivity using the slope of all variables, where a steep slope means a greater impact on the prediction. While the variables at the upper part have a greater impact on the prediction, those at the bottom generate smaller oscillation amplitudes for prediction with the tornado tool.

Result and Discussion

Temporal Distribution of $PM_{2.5}$ and $PM_{2.5}$-PAHs

In total, 504 air samples were collected at the monitoring site in Wuxi, and Table 1 summarizes the annual concentrations of $PM_{2.5}$ and 16 PAHs. The median $PM_{2.5}$ concentration decreased annually from 2016 (64.3 $\mu g/m^3$) to 2021 (34.0 $\mu g/m^3$), accompanied by a decrease in ∑PAHs levels. According to the PRC National Standard, the average 24-h ambient $PM_{2.5}$ concentration limit is 75 $\mu g/m^3$. The violation rates were 33.3% (2016), 19.0% (2017), 31.0% (2018), 15.5% (2019), 14.3% (2020), and 10.7% (2021). The median concentration of $PM_{2.5}$ in Wuxi was 64.3 $\mu g/m^3$ in 2016. This was 6.4 times higher than the $PM_{2.5}$ exposure limit of 10 $\mu g/m^3$ stipulated by WHO air quality guideline. Furthermore, 33.3% of the samples were higher than the PRC National Standard. A series of stringent emission control measures imposed in Wuxi are remarkable. An annual decrease in the concentration of $PM_{2.5}$, with a median of 34.0 $\mu g/m^3$ in 2021, reached the annual mean concentration limit of 35 $\mu g/m^3$. The $PM_{2.5}$-bound PAHs also showed a decreasing trend from 2016 to 2021. With the improvements and amendments of Air Pollution Prevention and Control Law of the People's Republic of China in 2018, several related regulations were put into practice in Wuxi. Industrial restructuring and energy structure reformation were implemented over time. Total industrial coal consumption

Table 1 Annual concentrations of 16 PAHs in $PM_{2.5}$ at sampling site

	2016	2017	2018	2019	2020	2021
$PM_{2.5}$ ($\mu g/m^3$)	64.3 (34.9–86.2)	50.6 (33.2–70.4)	57.9 (39.3–80.8)	44.4 (31.7–62.8)	38.9 (27.5–50.8)	34.0 (21.3–54.7)
Nap (ng/m^3)	0.13 (0.13–0.13)	0.13 (0.13–0.13)	0.13 (0.13–0.13)	0.13 (0.13–0.13)	0.13 (0.13–0.13)	0.13 (0.13–0.13)
Acy (ng/m^3)	0.08 (0.08–0.08)	0.08 (0.08–0.08)	0.08 (0.08–0.08)	0.08 (0.08–0.08)	0.08 (0.08–0.08)	0.08 (0.08–0.08)
Flu (ng/m^3)	0.03 (0.03–0.03)	0.03 (0.03–0.03)	0.03 (0.03–0.03)	0.03 (0.03–0.03)	0.03 (0.03–0.03)	0.03 (0.03–0.03)
Ace (ng/m^3)	0.23 (0.05–0.41)	0.22 (0.17–0.35)	0.17 (0.05–0.31)	0.05 (0.05–0.13)	0.05 (0.05–0.05)	0.05 (0.05–0.05)
Phe (ng/m^3)	0.06 (0.06–1.49)	0.88 (0.17–1.28)	1.00 (0.67–1.28)	0.42 (0.06–1.10)	0.06 (0.06–0.31)	0.84 (0.44–1.51)
Ant (ng/m^3)	0.05 (0.05–0.23)	0.05 (0.05–0.39)	0.05 (0.05–0.51)	0.05 (0.05–0.05)	0.09 (0.05–0.55)	0.24 (0.07–0.43)
Fla (ng/m^3)	0.05 (0.05–0.05)	0.05 (0.05–0.05)	0.05 (0.05–0.05)	0.05 (0.05–0.05)	0.05 (0.05–0.05)	0.05 (0.05–05)
Pyr (ng/m^3)	0.03 (0.03–1.59)	0.03 (0.03–0.03)	0.03 (0.03–0.03)	0.03 (0.03–0.03)	0.03 (0.03–0.03)	0.03 (0.03–1.02)
Chr (ng/m^3)	0.04 (0.04–0.97)	0.70 (0.04–1.42)	0.49 (0.04–0.78)	0.04 (0.04–0.09)	0.04 (0.04–0.09)	0.04 (0.04–0.04)
Baa (ng/m^3)	0.03 (0.03–1.67)	1.15 (0.03–2.04)	0.46 (0.03–0.98)	0.03 (0.03–0.36)	0.03 (0.03–0.22)	0.03 (0.03–0.03)
Bbf (ng/m^3)	0.03 (0.03–0.03)	0.03 (0.03–0.64)	0.03 (0.03–1.37)	1.11 (0.69–2.03)	0.36 (0.18–1.59)	0.28 (0.14–0.72)
Bkf (ng/m^3)	3.35 (3.35–4.62)	2.27 (0.89–2.99)	2.21 (1.45–2.80)	1.33 (0.82–3.07)	0.13 (0.07–1.26)	0.10 (0.06–0.26)
BaP (ng/m^3)	0.03 (0.03–0.73)	0.37 (0.03–1.69)	0.27 (0.21–0.65)	0.16 (0.09–0.30)	0.15 (0.07–0.29)	0.08 (0.03–0.29)
Dah (ng/m^3)	0.03 (0.03–0.35)	0.03 (0.03–0.73)	0.03 (0.03–0.03)	0.03 (0.03–0.03)	0.03 (0.03–0.03)	0.03 (0.03–0.05)
Bghi (ng/m^3)	1.27 (1.27–3.13)	1.63 (0.13–3.03)	1.23 (0.83–1.58)	0.54 (0.31–1.00)	0.36 (0.21–0.84)	0.58 (0.30–1.45)
Ind (ng/m^3)	0.04 (0.04–0.04)	0.04 (0.04–2.34)	0.04 (0.04–0.04)	0.04 (0.04–0.04)	0.04 (0.04–0.04)	0.04 (0.04–0.04)
∑PAHs (ng/m^3)	5.27 (5.27–14.4)	8.39 (0.43–17.8)	7.06 (5.90–12.43)	5.05 (3.33–9.18)	3.14 (1.70–5.26)	4.22 (2.70–5.12)
Rainfall (mm/h)	0.02 (0.00–3.10)	0.01 (0.00–1.67)	0.00 (0.00–1.50)	0.01 (0.00–4.20)	0.02 (0.00–2.60)	0.05 (0.00–1.68)

is decreasing year by year, and new energy vehicles achieve greater penetration (Shang et al. 2022). The substantial air quality optimization in 2020 and 2021 could be attributed to the COVID-19 pandemic (Qiu et al. 2023). The measures employed during the epidemic period, such as household isolation, shutdown and production stoppage, objectively improved the air quality of the city.

Moreover, the BaP concentration in 2017 was exceeded the recommended health-based standard of the EU at 1 ng/m^3; however, the annual concentration was consistent with China's National Standards at 1 ng/m^3 specified by the Ambient Air Quality Standards GB3095-2012. BaP is one of the common PAHs that is used as a proxy to estimate the toxicity of overall PAH levels. The carcinogenic, teratogenic, and mutagenic properties of BaP metabolites were confirmed, and are classified as class I carcinogens by the International Agency for Research on Cancer. Epidemiology studies have reported that BaP exposure is associated with the occurrence of human tumors including breast cancer, skin cancer, and lung cancer (Amadou et al. 2021; Magee and Forsberg 2021; Zhang et al. 2023). When cytochrome P450 enzymatically converts BaP, its metabolites may form toxic adducts with guanine, resulting in the disruption of normal DNA replication (Moorthy et al. 2015).

Among the 16 PAHs, Nap, Acy, Flu, Fla, Pyr, Dah, and Ind were seldom detected, whereas Phe, Baa, Bkf, BaP, and Bghi accounted for a large proportion of the PAH composition. Bkf (five rings) had the highest concentration between 2016 and 2019. Bbf (five rings) has increased since 2019, as shown in Fig. 2. Moreover, Bghi (six rings) was found to be a steady component, accounting for 11–19% during the observation period. Owing to semi-volatility, PAHs possessing 2–3 aromatic rings are predominant in the gaseous phase, while PAHs with four or more aromatic rings are dominant in the particulate phase (Wang et al. 2014). The dominant PAHs were 5–6 ring compounds, indicating a prominent contribution of vehicle exhaust. The 2–3 ring PAHs are generated by the pyrolysis of unburned fossil fuels, and four-ring PAHs are produced via coal/biomass combustion (Feng et al. 2021). Recently, the composition of $PM_{2.5}$-bound PAHs has demonstrated a trend of diversification, suggesting that pollution sources are also increasing in Wuxi.

Furthermore, the seasonal distribution variation of $PM_{2.5}$ and 16 PAHs were remarkable, as shown in Fig. 3. $PM_{2.5}$ concentrations in spring (63.3 ± 24.9 μg/m^3) and winter (69.1 ± 34.9 μg/m^3) were significantly higher than those in summer (43.3 ± 28.1 μg/m^3) and fall (39.4 ± 24.2 μg/m^3), and total $PM_{2.5}$-bound 16 PAHs concentration was higher in winter (15.4 ± 10.5 ng/m^3) than in other seasons (5.85 ± 3.95, 5.54 ± 4.05, and 5.97 ± 3.90 ng/m^3 for spring, summer, and fall, respectively). China has the highest PAH

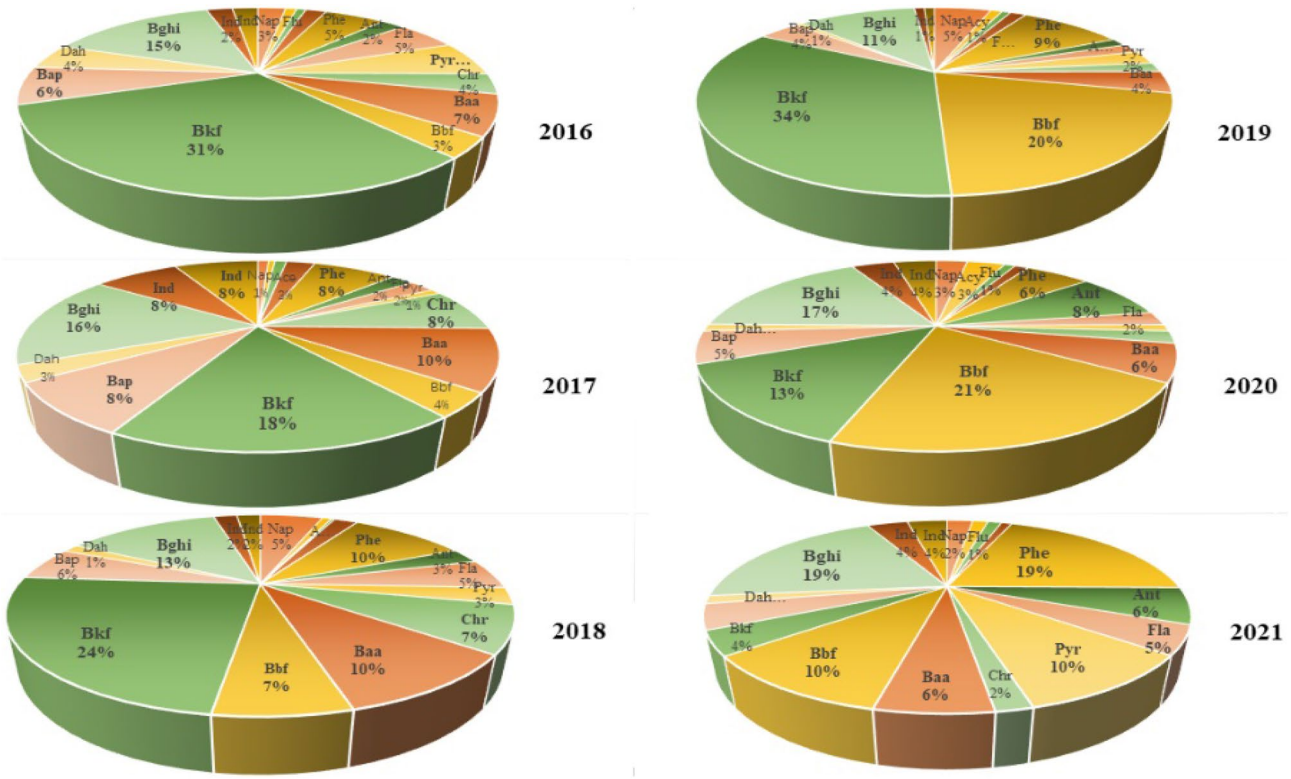

Fig. 2 Annual proportion of 16 PAHs in $PM_{2.5}$ samples

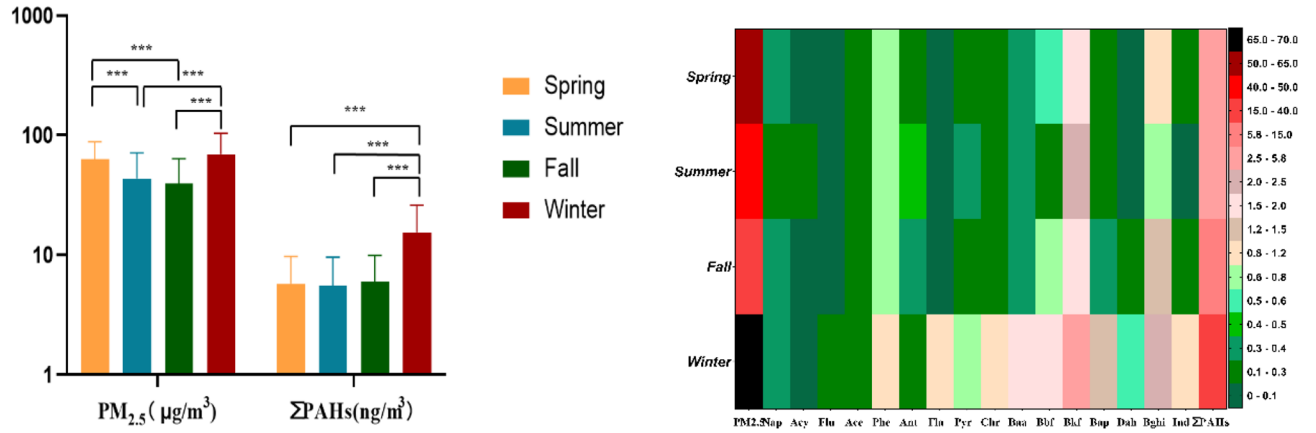

(a) Seasonal variation of PM2.5, and ∑PAHs (b) Concentration range of 16 PAHs and $PM_{2.5}$.

Fig. 3 Seasonal distribution difference of 16 PAHs and $PM_{2.5}$.*** means p value was less than 0.001

emissions globally and higher atmospheric PAH pollution is observed in winter than in other seasons (Shen et al. 2013) owing to its coal-dominant energy structure. The high PAH levels in winter can be attributed to the massive coal combustion emissions due to heating and meteorology parameters, such as temperature and humidity (Sun et al. 2022). The energy consumption structure, which has given priority to coal, will not markedly change in the future, and severe PAH contamination in winter will continue to increase.

Source Apportionment

To reduce PAH emissions, it is necessary to specify the primary emission sources. MDRs have been widely applied for $PM_{2.5}$-bound PAHs source apportionment. Typically, the diagnostic ratios of Ant/ (Ant + Phe), Fla/ (Fla + Pyr), Baa/ (Baa + Chr), Ind/ (Ind + Bghi), and BaP/ Bghi are used to confirm the contributions of various atmospheric PAHs sources. The details of the MDRs in the different years and seasons are listed in Table 2.

Considering the detection rate of PAHs, samples above the detection limit were selected for MDR calculation. The Ant/ (Ant + Phe) ratio is indicative of pyrogenic and petrogenic sources, and the Ant/ (Ant + Phe) ratio was higher than 0.1 from 2016 to 2021, indicating that pyrogenic sources were predominant. The Fla/ (Fla + Pyr) ratio is used as an indicator of petrogenic or unburned petroleum, fossil fuel, biomass, and coal combustion. Except for during 2021, the Fla/ (Fla + Pyr) ratio was typically greater than 0.5, which suggests emission from biomass and coal

Table 2 Details of MDRs values in temporal $PM_{2.5}$

	Ant/(Ant + Phe)	Fla/(Fla + Pyr)	Baa/(Baa + Chr)	Ind/(Ind + Bghi)	BaP/Bghi
2016	0.23 ± 0.12	0.66 ± 0.18	0.62 ± 0.10	0.27 ± 0.14	0.45 ± 0.27
2017	0.32 ± 0.08	0.60 ± 0.02	0.57 ± 0.11	0.53 ± 0.14	0.75 ± 0.92
2018	0.35 ± 0.05	0.58 ± 0.08	0.55 ± 0.10	0.68 ± 0.05	0.51 ± 0.63
2019	0.36 ± 0.06	0.50 ± 0.01	0.75 ± 0.07	0.46 ± 0.18	0.33 ± 0.17
2020	0.27 ± 0.08	0.66 ± 0.12	0.69 ± 0.13	0.44 ± 0.08	0.47 ± 0.12
2021	0.31 ± 0.16	0.46 ± 0.08	0.79 ± 0.09	0.36 ± 0.06	0.20 ± 0.07
Spring	0.34 ± 0.12	0.74 ± 0.16	0.60 ± 0.11	0.70 ± 0.07	0.38 ± 0.43
Summer	0.33 ± 0.13	0.56 ± 0.20	0.51 ± 0.11	0.21 ± 0.13	0.26 ± 0.14
Fall	0.31 ± 0.12	0.62 ± 0.18	0.58 ± 0.10	0.42 ± 0.13	0.33 ± 0.49
Winter	0.29 ± 0.17	0.54 ± 0.09	0.66 ± 0.12	0.40 ± 0.15	0.75 ± 0.96
	< 0.1 = petrogenic > 0.1 = pyrogenic	< 0.4 = petrogenic/unburned petroleum 0.4–0.5 = fossil fuel combustion > 0.5 = biomass and coal combustion	< 0.2 = petrogenic 0.2–0.35 = petroleum combustion > 0.35 = biomass and coal combustion	< 0.2 = petrogenic 0.2–0.5 = petroleum combustion > 0.5 = biomass and coal combustion	< 0.6 = nontraffic > 0.6 = traffic

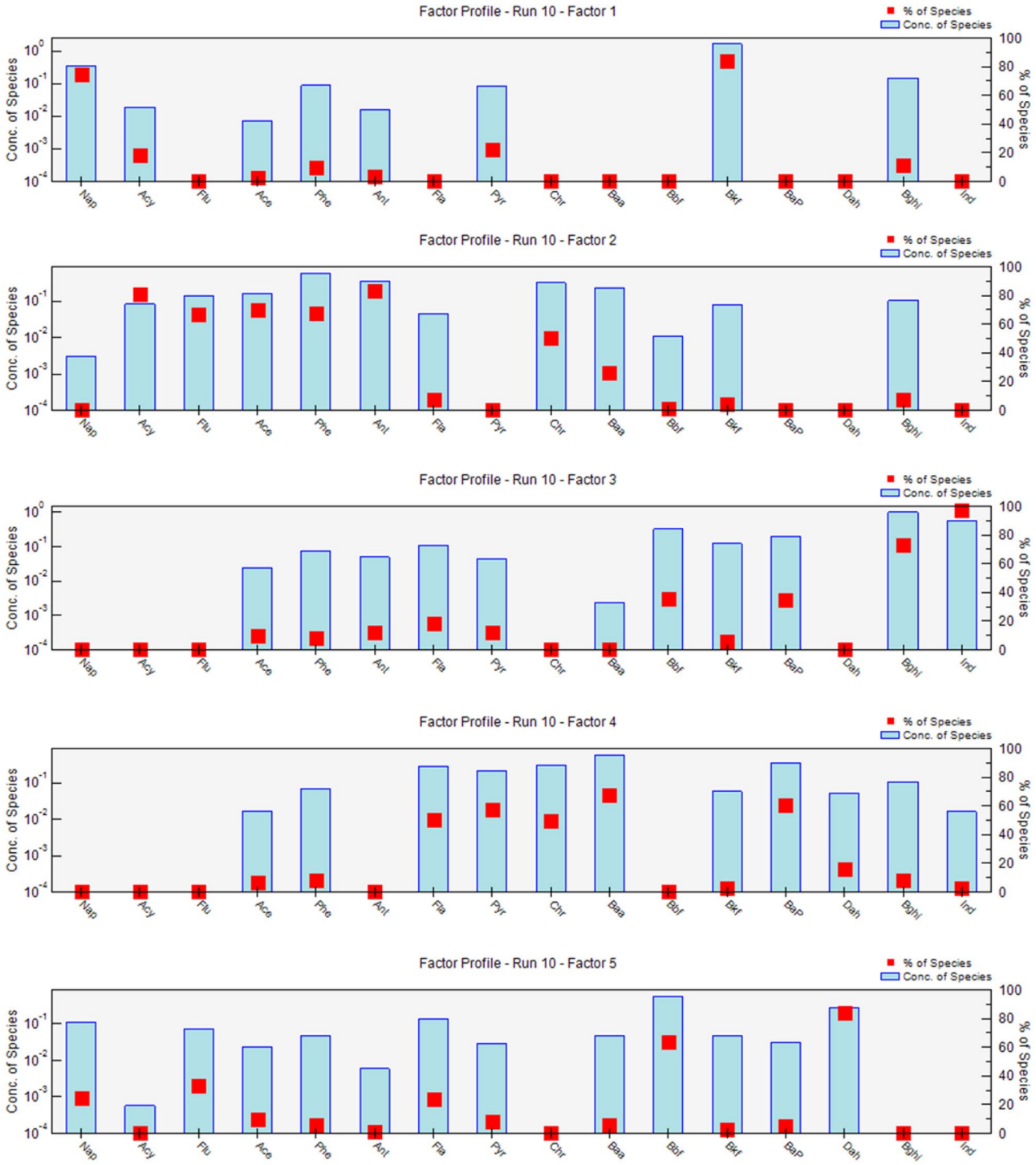

Fig. 4 PMF species profiles of 16 PAHs which constitute the 5 factors

combustion. Moreover, the Baa/ (Baa + Chr) ratio was higher than 0.35 which indicated emission from biomass and coal combustion. For the Ind/ (Ind + Bghi) ratio, the majority of the samples were between 0.2 and 0.5, which represent petroleum combustion emission. However, these ratios were higher than 0.5, in 2018 (0.68 ± 0.05) and in spring (0.70 ± 0.07) when they were grouped by season. The BaP/ Bghi ratios used to distinguish traffic sources indicated less traffic pollution emissions in this area.

The PMF species profiles are illustrated in Fig. 4. Factor 1 is dominated by Nap and Bkf. Considering that Nap is more likely to be detected in gaseous phases than $PM_{2.5}$, and Bkf is considered to originate from diesel combustion (Yancheshmeh et al. 2014; Shen et al. 2019). Factor 1 was defined as diesel combustion. Factor 2 is dominated by Acy, Flu, Ace, Phe, Ant, and Chr. Low molecular weight PAHs play a leading role here as they are primarily derived from low-temperature combustion (Wang et al. 2010), such as coal combustion. They are also likely to decrease with the decreasing diameter of PMs (Wang et al. 2018). Therefore, Factor 2 was defined as coal combustion. Factor 3 was dominated by Bghi and Ind, which are generated from incomplete gasoline combustion and are the markers of high traffic flow in cities (Zaragoza-Ojeda et al. 2022). Therefore, Factor 3 was defined as gasoline emissions. Factor 4 was dominated by Fla, Pyr, Chr, Baa, and BaP. Chr and Baa are good tracers of biomass burning. The detectable BaP is typically derived from the combustion of organic matter and natural sources, such as forest fires and volcanic eruptions (Ofori et al. 2020; Wu et al. 2022). Factor 4 is defined as biomass burning. Factor 5 was dominated by Bbf and Dah. Dah was seldom detected in the $PM_{2.5}$ samples. A remarkably high Bbf/ Bkf ratio was observed in snack-street boiling, which was attributed to cooking fumes (Liu et al., 2018). Furthermore, Bbf was selected by the EU Scientific Committee on Food as one of the most suitable indicators of carcinogenic PAHs in food (EU 2011). Hence, Factor 5 was defined as cooking. Cooking emissions, known as the cooking-like organic aerosol factor, are an important source of organic aerosols. Cooking emissions were found to account for 90% of PAHs on average, nine times higher than that of traffic (10%) (Lin et al. 2022).

The concentrations of $PM_{2.5}$ and $PM_{2.5}$-bound PAHs were significantly correlated to local precipitation. The relationship of $PM_{2.5}$ and 16 $PM_{2.5}$-bound PAHs with local precipitation was also investigated. The precipitation data shown in Table 1 were obtained from the European Centre for Medium-Range Weather Forecasts (Global Modeling and Assimilation Office 2015). Multilevel regression modeling tested the association between $PM_{2.5}$ and 16 $PM_{2.5}$-bound PAHs with precipitation. Both $PM_{2.5}$ and 16 $PM_{2.5}$-bound PAHs were significantly negatively associated with local precipitation over a six years period: β coefficient: −18.029, 95% confidence interval: (−24.408, −11.652) with $p < 0.001$ for $PM_{2.5}$, and β coefficient: −2.880, 95% confidence interval: (−4.456, −1.305) with $p < 0.001$ for $PM_{2.5}$-bound PAHs. Our results were consistent with those of previous studies that showed air pollutants were reduced by rainfall scavenging, with the greatest reduction observed in $PM_{2.5}$ (Lv et al. 2021).

Spatial Distribution Variations of $PM_{2.5}$ and PAHs Levels

A literature review was conducted to understand the spatial distribution differences of the EPA priority 16 PAHs. Studies that reported data on 16 PAHs in atmospheric samples were included in the review. The exclusion criteria were as follows: (1) sampling dates earlier than 2016 or later than 2021; (2) sampling sites that were contaminated areas; (3) mean, standard deviation, and sample sizes that were not found in the literature; and (4) the 16 PAH types that were not the same as those in the current study. Eleven studies met the criteria described above and the results are presented in Fig. 5. Individual *t*-tests were performed between relevant data and the present study according to the sampling time for $PM_{2.5}$ and ∑PAHs. The $PM_{2.5}$ concentration of the study area was significantly different from that of Jamshedpur City and Ranchi of India (more heavily polluted than Wuxi), Shanghai of China (superior to Wuxi), and six provinces of Thailand (superior to Wuxi). The ∑PAH distributions of Seoul, Korea, Arequipa of Peru, and six provinces of Thailand were not significantly different from that in the present study. The ∑PAHs concentrations in other areas were higher than that in the present study, except for Shanghai, China ($p < 0.01$). The details of the $PM_{2.5}$-bound PAHs are listed in Table S3. Furthermore, PAH levels were not always associated with $PM_{2.5}$, and no significant differences were observed between Wuxi and Eastern India, Changchun, Tehran, and Dalian; however, the distributions of $PM_{2.5}$, were distinctly different. PAHs are also regulated by meteorological processes, such as the size distribution of particles, particle diameter, and particle density (Wang et al. 2019).

Health Risk Assessment of Membrane-Captured PAHs

Based on the health risk assessment model and toxicity parameters, the ILCR of children, teenagers, and adults exposed to PAHs ($PM_{2.5}$) in Wuxi City was calculated using Crystal Ball. The median TEQ was 0.70 for a total of 15 PAHs and TEQ conformed to the lognormal distribution, as shown in Fig. S2(a). Fig. S2(b) illustrates the individual TEQ of each PAH. The TEQ of BaP (0.178) was the highest, followed by that of Bkf (0.090), Dah (0.048), Ind (0.034), and Baa (0.014).

The ILCR calculated using Eq. (2) was analyzed using a dynamic simulation. Monte Carlo analysis has been widely applied in uncertainty model. Through 10,000 simulations, the medians of the ILCR for long-term exposure to PAHs were 2.74E−8 (max: 2.00E−6), 1.98E−8 (max: 3.64E−6), and 1.71E−7 (max: 2.21E−5) for children, teenagers, and adults, respectively. According to the results, ILCR can be divided into four categories: very low

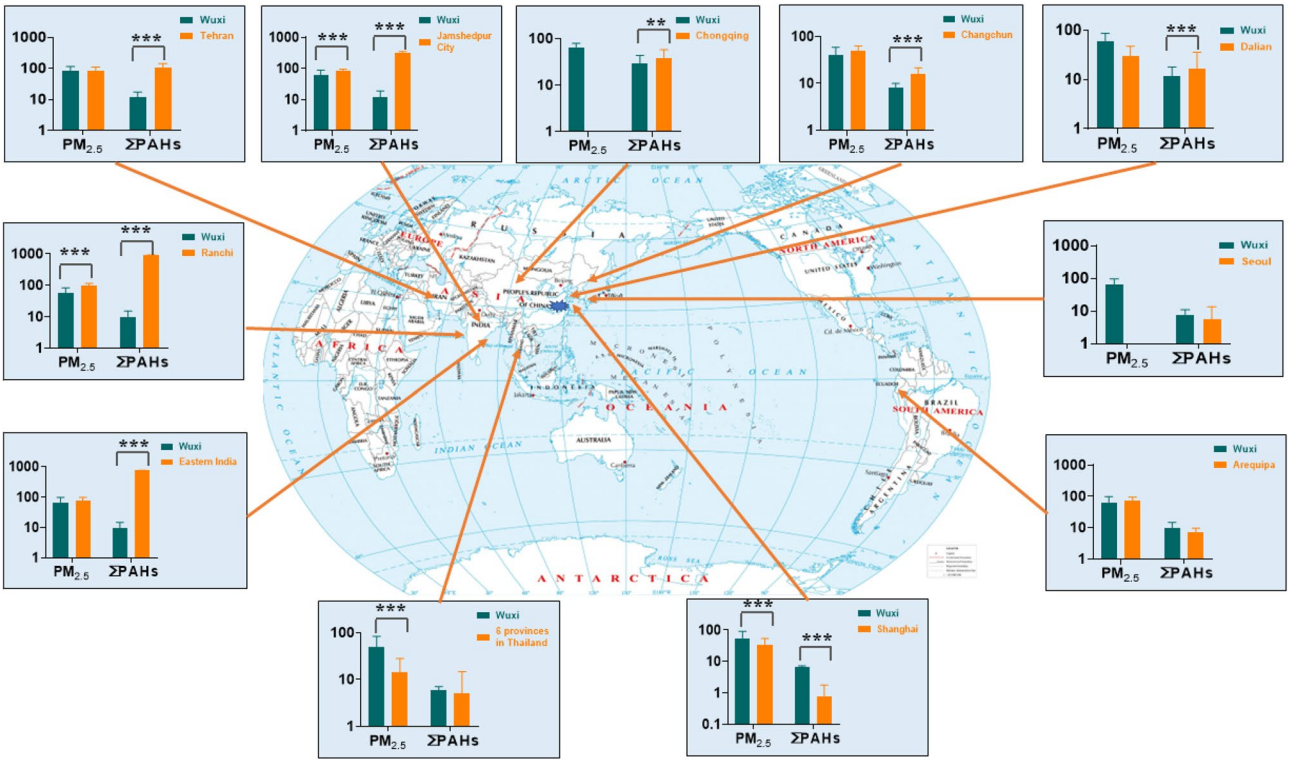

Fig. 5 Spatial distribution variations of $PM_{2.5}$ and 16 PAHs. ** means *p* value was less than 0.01, *** means *p* value was less than 0.001

(ILCR < 1.0E−6), low (1.0E−6 < ILCR < 1.0E−4), medium (1.0E−4 < ILCR < 1.0E−3) and high carcinogenic risk (ILCR > 1.0E−3). This is a low carcinogenic risk of PAH air pollution in this area; however, the maximum ILCR for adults exceeded the EPA recommended limit in the winter. Other studies reported that adult ILCR exceeded 1.0E−6 in industrial area of northern China, and high cancer risks exceeded EPA recommended limit in Jinan, located in the northern China (Jiang et al. 2022; Yu et al. 2022). In India, the TEQ ranged between 0.24 and 94.13 while the ILCR ranged between 1.0E−5 and 1.0E−3, representing a relative high cancer risk (Ekka et al. 2021). PAHs were also reported in soils and water which could accumulate and pose a threat to grain, fish, and vegetables (Sonego et al. 2022; Zhang et al. 2022). Considering the multiple exposure pathways, the risk of adult exposure to PAHs cannot be neglected.

Furthermore, the Spider chart and Tornado tool in Crystal Ball were employed for sensitivity analysis to identify prominent contaminants, as shown in Fig. 6. Evidently, body weight had a greater negative effect on prediction, while ingestion rate and exposure duration had a positive effect. Among the 15 PAHs, BaP, Bkf, and Dah significantly contributed to carcinogenic toxicity. The consequences for children and teenagers were consistent with those for adults, which can be found in the Supplementary Information. BaP is a well-known highly toxic and carcinogenic compound. Recent studies have also reported that Bkf also is the most important contributor to the aryl hydrocarbon receptor activation which participates in the mechanism of $PM_{2.5}$-induced cardiovascular disease, followed by Bbf and Dah (Ho et al. 2022; Ma et al. 2022). Bkf was found to adversely affect cell viability and necrosis in the placental cell line, indicating potential reproductive toxicity (Jo et al. 2022). Bkf was abundant in several environments, even in Arctic seas (Lakhmanov et al. 2022; Zonkpoedjre et al. 2022). Therefore, it is worthwhile to focus on Bkf pollution.

To accurately evaluate the associations between the parameters and ILCR prediction, a scatter plot of the sensitivity analysis was used to obtain the correlation coefficient, as shown in Fig. 7. The exposure duration, ingestion rate, BaP, Bkf, and Dah were positively correlated, with *R* values of 0.6312, 0.1353, 0.4573, 0.3043, and 0.1600, respectively. In contrast, body weight was inversely related to ILCR prediction, with an *R* value of −0.1359. Scatter plots of the relationships for children and teenagers are provided in the Supplementary Information.

Conclusion

Long-term atmospheric surveillance of 16 $PM_{2.5}$-bound PAHs was conducted from 2016 to 2021 in Wuxi City. Based on our monitoring data, $PM_{2.5}$ pollution was degraded

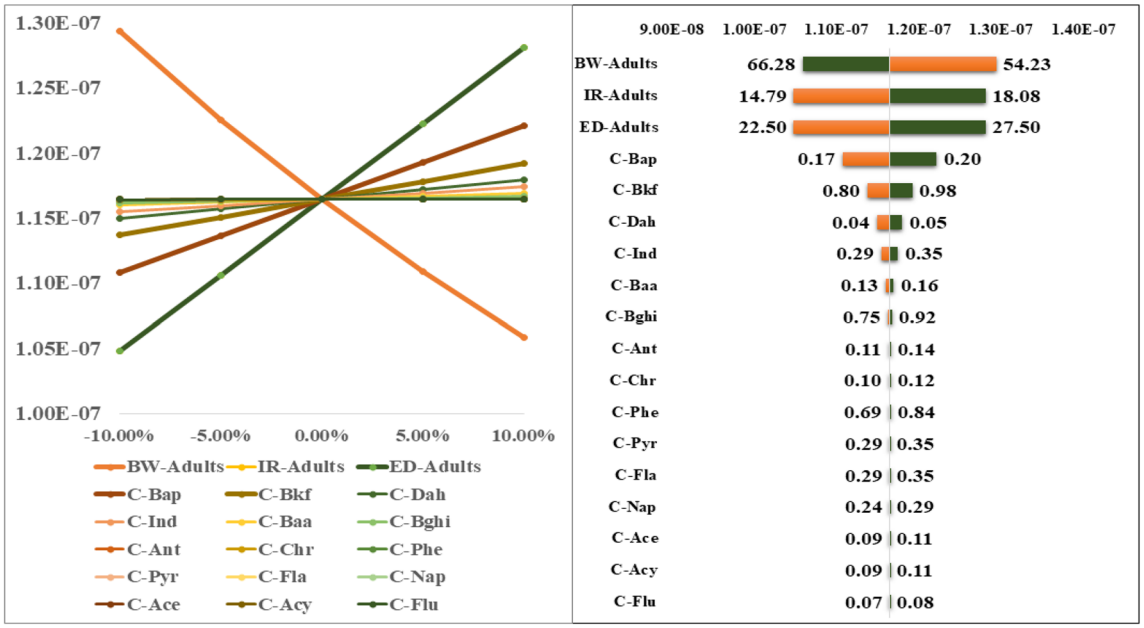

Fig. 6 Sensitivity analysis for adults ILCR prediction. IR is the inhalation rate ($m^3 \cdot day^{-1}$), ED is the exposure duration (years), BW is the body weight (kg)

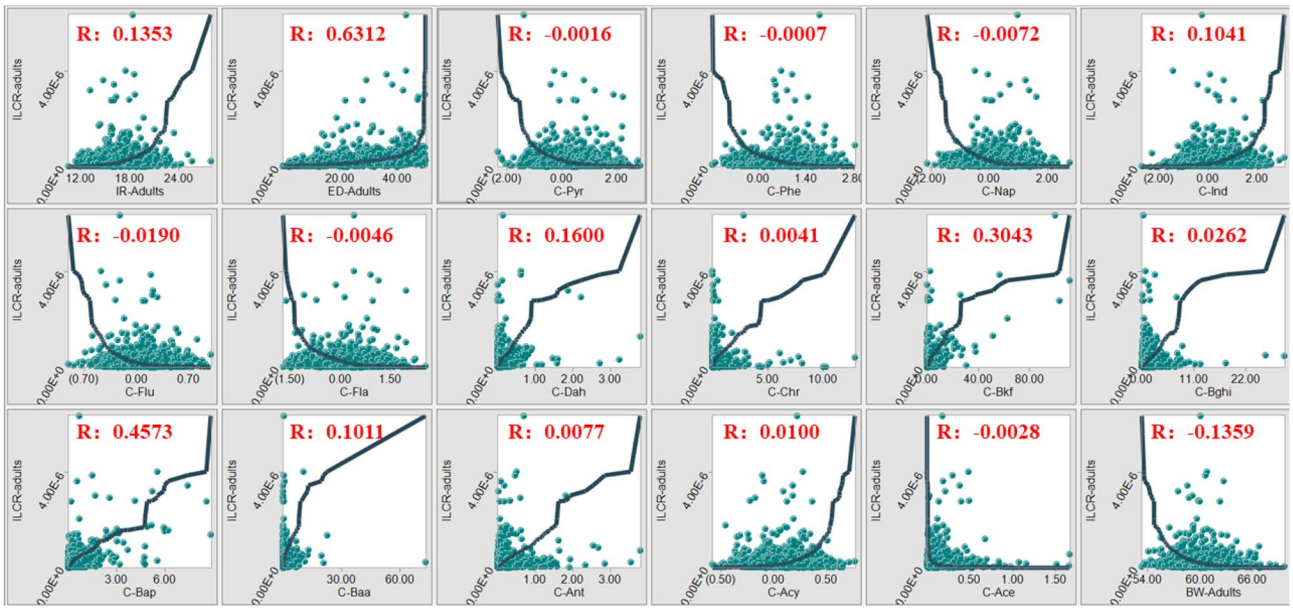

Fig. 7 Scatter plot of sensitivity analysis for adults ILCR prediction. IR is the inhalation rate ($m^3 \cdot day^{-1}$), ED is the exposure duration (years), BW is the body weight (kg)

annually, and violations were primarily observed in winter. BaP exceeded the EU-recommended health-based standard in 2017. Owing to the prior energy consumption structure using coal, 16 PAHs were three times higher in winter than in the other seasons. Moreover, there were significant spatial distribution differences in PAHs. High-molecular-weight PAHs, including Bkf, BaP, and Bghi, were the dominant components, indicating diesel combustion, gasoline emissions, and biomass burning when applying MDR and PMF analyses. The ILCR resulting from respiratory exposure to PAHs was acceptable to local citizens, with maximum value of 2.00E−6, 3.64E−6, and 2.21E−5 for children, teenagers, and adults, respectively. BaP, Bkf, and Dah had a positive impact on ILCR predictions. Our study provides a detailed

profile of $PM_{2.5}$-bound PAHs pollution and its health effects on local residents. However, air pollution during winter should not be neglected. The toxicities and carcinogenicity of long-term exposure to $PM_{2.5}$ and the dominant PAHs also require further clarification.

Supplementary Information The online version contains supplementary material available at https://doi.org/10.1007/s12403-023-00572-x.

Acknowledgements The authors appreciate the funding support and the support of the colleagues. We would also like to thank Editage (www.editage.cn) for English language editing.

Author contributions Keqin Wu: Conceptualization, Methodology, Software, Writing; Yuyang Yao: Methodology, Software; Yuanhua Meng: Data Curation, Writing—Review & Editing; Xuhui Zhang: sample collection; Run Zhou: Writing—Reviewing & Editing; Wenwei Liu: Writing- Reviewing and Editing, Funding acquisition; Xinliang Ding: Writing- Reviewing and Editing, Funding acquisition, Project administration.

Funding This study was supported by the Top Talent Support Program for young and middle-aged people of the Wuxi Health Commission [Grant Numbers BJ2020095 and HB2020098], Wuxi Science and Technology Bureau project [Grant Number Y20212040], Medical Key Discipline Program of Wuxi Health Commission [Grant Numbers LCZX2021006 and CXTD2021004], and Scientific Research Project of Wuxi Health Commission [Grant Number M202047].

Data availability The datasets generated during the current study are available from the corresponding author on reasonable request.

Declarations

Conflict of interest The authors declare that they have no known competing financial interests or personal relationships that could influence the work reported in this paper.

References

Air Quality Standards. European Commission. [(accessed on 16 December 2019)]; Available online: https://ec.europa.eu/environment/air/quality/standards.htm.

Amadou A, Praud D, Coudon T, Deygas F, Grassot L, Faure E, Couvidat F, Caudeville J, Bessagnet B, Salizzoni P, Gulliver J, Leffondré K, Severi G, Mancini FR, Fervers B (2021) Risk of breast cancer associated with long-term exposure to benzo[a]pyrene (BaP) air pollution: Evidence from the French E3N cohort study. Environ Int 149:106399. https://doi.org/10.1016/j.envint.2021.106399

Andersson JT, Achten C (2015) Time to say goodbye to the 16 EPA PAHs? Toward an up-to-date use of PACs for environmental purposes. Polycyclic Aromat Compd 35(2–4):330–354. https://doi.org/10.1080/10406638.2014.991042

Berumen-Rodríguez AA, Díaz de León-Martínez L, Zamora-Mendoza BN, Orta-Arellanos H, Saldaña-Villanueva K, Barrera-López V, Gómez-Gómez A, Pérez-Vázquez FJ, Díaz-Barriga F, Flores-Ramírez R (2021) Evaluation of respiratory function and biomarkers of exposure to mixtures of pollutants in brick-kilns workers from a marginalized urban area in Mexico. Environ Sci Pollut Res Int 28(47):67833–67842. https://doi.org/10.1007/s11356-021-15375-3

Che C, Li J, Dong F, Zhang C, Liu L, Sun X, Ma L, Qi H, Wang K (2020) Seasonal characteristic composition of inorganic elements and polycyclic aromatic hydrocarbons in atmospheric fine particulate matter and bronchoalveolar lavage fluid of COPD patients in Northeast China. Respir Med 171:106082. https://doi.org/10.1016/j.rmed.2020.106082

Chen Q, Zhang J, Xu Y, Sun H, Ding Z (2020) Associations between individual perceptions of PM2.5 pollution and pulmonary function in Chinese middle-aged and elderly residents. BMC Public Health 20(1):899. https://doi.org/10.1186/s12889-020-08713-6

Diggs DL, Huderson AC, Harris KL, Myers JN, Banks LD, Rekhadevi PV, Niaz MS, Ramesh A (2011) Polycyclic aromatic hydrocarbons and digestive tract cancers: a perspective. J Environ Sci Health Part C Environ Carcinog Ecotoxicol Rev 29(4):324–357. https://doi.org/10.1080/10590501.2011.629974

Ekka S, Sahu SK, Dwivedi S, Khuman SN, Das S, Gaonkar O, Chakraborty P (2021) Seasonality, atmospheric transport and inhalation risk assessment of polycyclic aromatic hydrocarbons in PM2.5 and PM10 from industrial belts of Odisha, India. Environ Geochem Health. https://doi.org/10.1007/s10653-021-01128-1

US EPA (2017) Toxicological Review of Benzo[a] pyrene executive summary [CASRN 50-32-8]. Integrated Risk Information System, National Center for Environmental Assessment, Office of Research and Development, U.S. Environmental Protection Agency, Washington, DC

European Union Commission Regulation No 835/2011 of 19 August 2011 amending Regulation (EC) No 1881/2006 as regards maximum levels for polycyclic aromatic hydrocarbons in foodstuffs Official Journal of the European, L215 (2011), pp. 4–8

Fan X, Chen Z, Liang L, Qiu G (2019) Atmospheric PM2.5-bound polycyclic aromatic hydrocarbons (PAHs) in Guiyang City, Southwest China: concentration, seasonal variation, sources and health risk assessment. Arch Environ Contam Toxicol 76(1):102–113. https://doi.org/10.1007/s00244-018-0563-5

Fang B, Zhang L, Zeng H, Liu J, Yang Z, Wang H, Wang Q, Wang M (2020) PM2.5-Bound polycyclic aromatic hydrocarbons: sources and health risk during non-heating and heating periods (Tangshan, China). Int J Environ Res Public Health 17(2):483. https://doi.org/10.3390/ijerph17020483

Feng T, Wang F, Yang F, Li Z, Lu P, Guo Z (2021) Carbonaceous aerosols in urban Chongqing, China: seasonal variation, source apportionment, and long-range transport. Chemosphere 285:131462. https://doi.org/10.1016/j.chemosphere.2021.131462

Froehner S, Maceno M, Machado KS, Malheiros A (2010) Polycyclic aromatic hydrocarbons (PAHs) in airborne particulate matter in Curitiba, Brazil and benzo(a)pyrene toxic equivalency factors (TEFs). J Environ Sci Health Part A Toxic/Hazard Subst Environ Eng 45(11):1347–1352. https://doi.org/10.1080/10934529.2010.500889

Ho CC, Wu WT, Lin YJ, Weng CY, Tsai MH, Tsai HT, Chen YC, Yet SF, Lin P (2022) Aryl hydrocarbon receptor activation-mediated vascular toxicity of ambient fine particulate matter: contribution of polycyclic aromatic hydrocarbons and osteopontin as a biomarker. Part Fibre Toxicol 19(1):43. https://doi.org/10.1186/s12989-022-00482-x

Hsu SC, Chang JH, Lee CL, Huang WC, Hsu YP, Liu CT, Jean SS, Huang SK, Hsu CW (2020) Differential time-lag effects of ambient PM2.5 and PM2.5-bound PAHs on asthma emergency department visits. Environ Sci Pollut Res Int 27(34):43117–43124. https://doi.org/10.1007/s11356-020-10243-y

Idowu O, Semple KT, Ramadass K, O'Connor W, Hansbro P, Thavamani P (2019) Beyond the obvious: environmental health implications of polar polycyclic aromatic hydrocarbons. Environ Int 123:543–557. https://doi.org/10.1016/j.envint.2018.12.051

Jiang Q, Zhang X, Liu T, Shi J, Gu X, Xiao J, Fang J (2022) Assessment of the temporal variability and health risk of atmospheric

particle-phase polycyclic aromatic hydrocarbons in a northeastern city in China. Environ Sci Pollut Res Int. https://doi.org/10.1007/s11356-022-20378-9

Jo YS, Ko HS, Kim AY, Jo HG, Kim WJ, Choi SK (2022) Effects of polycyclic aromatic hydrocarbons on the proliferation and differentiation of placental cells. Reprod Biol Endocrinol 20(1):47. https://doi.org/10.1186/s12958-022-00920-7

Kang M, Kim K, Choi N, Kim YP, Lee JY (2020) Recent occurrence of PAHs and n-Alkanes in PM2.5 in Seoul, Korea and characteristics of their sources and toxicity. Int J Environ Res Public Health 17(4):1397. https://doi.org/10.3390/ijerph17041397

Kim KH, Jahan SA, Kabir E, Brown RJ (2013) A review of airborne polycyclic aromatic hydrocarbons (PAHs) and their human health effects. Environ Int 60:71–80. https://doi.org/10.1016/j.envint.2013.07.019

Lakhmanov DE, Kozhevnikov AY, Pokryshkin SA, Semiletov IP, Kosyakov DS (2022) Polycyclic aromatic hydrocarbons in the Siberian Arctic seas sediments. Mar Pollut Bull 180:113741. https://doi.org/10.1016/j.marpolbul.2022.113741

Le Goff M, Lagadic-Gossmann D, Latour R, Podechard N, Grova N, Gauffre F, Chevance S, Burel A, Appenzeller B, Ulmann L, Sergent O, Le Ferrec E (2019) PAHs increase the production of extracellular vesicles both in vitro in endothelial cells and in vivo in urines from rats. Environ Pollut 255(Pt 1):113171. https://doi.org/10.1016/j.envpol.2019.113171

Lin C, Huang RJ, Duan J, Zhong H, Xu W (2022) Polycyclic aromatic hydrocarbons from cooking emissions. Sci Total Environ 818:151700. https://doi.org/10.1016/j.scitotenv.2021.151700

Lou CR, Liu HY, Li YF, Li YL (2016) Socioeconomic drivers of PM2.5 in the accumulation phase of air pollution episodes in the Yangtze River Delta of China. Int J Environ Res Public Health 13(10):928. https://doi.org/10.3390/ijerph13100928

Lv M, Li Z, Jiang Q, Chen T, Wang Y, Hu A, Cribb M, Cai A (2021) Contrasting trends of surface PM2.5, O3, and NO_2 and their relationships with meteorological parameters in typical coastal and inland cities in the Yangtze River Delta. Int J Environ Res Public Health 18(23):12471. https://doi.org/10.3390/ijerph182312471

Ma D, Li G, He F (2021) Exploring PM2.5 environmental efficiency and its influencing factors in China. Int J Environ Res Public Health 18(22):12218. https://doi.org/10.3390/ijerph182212218

Ma Q, Liu Y, Yang X, Guo Y, Xiang T, Wang Y, Yan Y, Li D, Nie T, Li Z, Qu G, Jiang G (2022) Effect-directed analysis for revealing aryl hydrocarbon receptor agonists in sediment samples from an electronic waste recycling town in China. Environ Pollut 308:119659. https://doi.org/10.1016/j.envpol.2022.119659

Magee BH, Forsberg ND (2021) Testing the validity of a proposed dermal cancer slope factor for Benzo[a]pyrene. Regul Toxicol Pharmacol 120:104852. https://doi.org/10.1016/j.yrtph.2020.104852

Mao M, Sun H, Zhang X (2020) Air pollution characteristics and health risks in the Yangtze River Economic Belt, China during winter. Int J Environ Res Public Health 17(24):9172. https://doi.org/10.3390/ijerph17249172

Global Modeling and Assimilation Office (GMAO) (2015), MERRA-2 tavg1_2d_lnd_Nx, tavg1_2d_rad_Nx, tavg1_2d_slv_Nx: 2d,1-Hourly, Time-Averaged, Single-Level, Assimilation, Diagnostics V5.12.4 (M2T1NXSLV), Land Surface Diagnostics V5.12.4 (M2T1NXLND), Radiation Diagnostics V5.12.4 (M2T1NXRAD), Greenbelt, MD, USA, Goddard Earth Sciences Data

Moorthy B, Chu C, Carlin DJ (2015) Polycyclic aromatic hydrocarbons: from metabolism to lung cancer. Toxicol Sci 145(1):5–15. https://doi.org/10.1093/toxsci/kfv040

Nagato EG (2018) PAHs and NPAHs in airborne particulate matter: initial formation and atmospheric transformations. In: Hayakawa K (ed) Polycyclic aromatic hydrocarbons. Springer, Singapore

Nisbet IC, LaGoy PK (1992) Toxic equivalency factors (TEFs) for polycyclic aromatic hydrocarbons (PAHs). Regul Toxicol Pharmacol RTP 16(3):290–300. https://doi.org/10.1016/0273-2300(92)90009-x

Ofori SA, Cobbina SJ, Doke DA (2020) The occurrence and levels of polycyclic aromatic hydrocarbons (PAHs) in African environments-a systematic review. Environ Sci Pollut Res Int 27(26):32389–32431. https://doi.org/10.1007/s11356-020-09428-2

Paatero P (1997) Least squares formulation of robust non-negative factor analysis. Chemom Intell Lab Syst 37:23–35. https://doi.org/10.1016/S0169-7439(96)00044-5

Paatero P, Tapper U (1994) Positive matrix factorization: a non-negative factor model with optimal utilization of error estimates of data values. Environmetrics 5:111–126

Qiu J, Li P, You C, Fan H (2023) Research of the impact of economic decline on air quality in Wuhan under COVID-19 epidemic. PLoS One 18(3):e0282706. https://doi.org/10.1371/journal.pone.0282706

Ravindra K, Sokhi R, Van Grieken R (2008) Atmospheric polycyclic aromatic hydrocarbons: source attribution, emission factors and regulation. Atmos Environ 42(13):2895–2921. https://doi.org/10.1016/j.atmosenv.2007.12.010

Rezaei F, Kakooei H, Ahmadkhaniha R, Azam K, Omidi L, Shahtaheri SJ (2018) Inhalation exposure and health risks for newsagents exposed to atmospheric polycyclic aromatic hydrocarbons in Tehran, Iran. Urban Clim 24:796–802. https://doi.org/10.1016/j.uclim.2017.10.003

Shang Y, Lyu G, Mi Z (2022) Green technology transfer, environmental regulation, and regional green development chasm: based on the empirical evidence from Yangtze River Delta. Int J Environ Res Public Health 19(21):13925. https://doi.org/10.3390/ijerph192113925

Shen H, Huang Y, Wang R, Zhu D, Li W, Shen G, Wang B, Zhang Y, Chen Y, Lu Y, Chen H, Li T, Sun K, Li B, Liu W, Liu J, Tao S (2013) Global atmospheric emissions of polycyclic aromatic hydrocarbons from 1960 to 2008 and future predictions. Environ Sci Technol 47(12):6415–6424. https://doi.org/10.1021/es400857z

Shen R, Liu Z, Chen X, Wang Y, Wang L, Liu Y, Li X (2019) Atmospheric levels, variations, sources and health risk of PM2.5-bound polycyclic aromatic hydrocarbons during winter over the North China Plain. Sci Total Environ 655:581–590. https://doi.org/10.1016/j.scitotenv.2018.11.220

Sonego E, Bhattarai B, Duedahl-Olesen L (2022) Detection of nitrated, oxygenated and hydrogenated polycyclic aromatic compounds in smoked fish and meat products. Foods 11(16):2446. https://doi.org/10.3390/foods11162446

Stanišić S, Perišić M, Jovanović G, Milićević T, Romanić SH, Jovanović A, Šoštarić A, Udovičić V, Stojić A (2021) The PM2.5-bound polycyclic aromatic hydrocarbon behavior in indoor and outdoor environments, part I: Emission sources. Environ Res 193:110520. https://doi.org/10.1016/j.envres.2020.110520

Sun J, Shen Z, Zhang T, Kong S, Zhang H, Zhang Q, Niu X, Huang S, Xu H, Ho KF, Cao J (2022) A comprehensive evaluation of PM2.5-bound PAHs and their derivative in winter from six megacities in China: Insight the source-dependent health risk and secondary reactions. Environ Int 165:107344. https://doi.org/10.1016/j.envint.2022.107344

Toriba A, Hayakawa K (2021) What is necessary for next-generation atmospheric environmental standards? Recent research trends for PM2.5-bound polycyclic aromatic hydrocarbons and their derivatives. Biomed Chromatogr BMC 35(1):e5038. https://doi.org/10.1002/bmc.5038

Wang X, Yang H, Gong P, Zhao X, Wu G, Turner S, Yao T (2010) One century sedimentary records of polycyclic aromatic hydrocarbons,

mercury and trace elements in the Qinghai Lake, Tibetan Plateau. Environ Pollut 158(10):3065–3070. https://doi.org/10.1016/j.envpol.2010.06.034

Wang J, Geng NB, Xu YF, Zhang WD, Tang XY, Zhang RQ (2014) PAHs in PM2.5 in Zhengzhou: concentration, carcinogenic risk analysis, and source apportionment. Environ Monit Assess 186(11):7461–7473. https://doi.org/10.1007/s10661-014-3940-1

Wang S, Zhou C, Wang Z, Feng K, Hubacek K (2017) The characteristics and drivers of fine particulate matter (PM2.5) distribution in China. J Clean Prod 142:1800–1809

Wang R, Liu G, Sun R, Yousaf B, Wang J, Liu R, Zhang H (2018) Emission characteristics for gaseous- and size-segregated particulate PAHs in coal combustion flue gas from circulating fluidized bed (CFB) boiler. Environ Pollut 238:581–589. https://doi.org/10.1016/j.envpol.2018.03.051

Wang Y, Zhang Q, Zhang Y, Zhao H, Tan F, Wu X, Chen J (2019) Source apportionment of polycyclic aromatic hydrocarbons (PAHs) in the air of Dalian, China: correlations with six criteria air pollutants and meteorological conditions. Chemosphere 216:516–523. https://doi.org/10.1016/j.chemosphere.2018.10.184

Wang Q, Fang J, Shi W, Dong X (2020) Distribution characteristics and policy-related improvements of PM2.5 and its components in six Chinese cities. Environ Pollut 266(Pt 3):115299. https://doi.org/10.1016/j.envpol.2020.115299

WHO (World Health Organization) (2003) Polynuclear aromatic hydrocarbons in drinking-water. Background document for development of WHO Guidelines for Drinking-water Quality

Wu M, Luo J, Huang T, Lian L, Chen T, Song S, Wang Z, Ma S, Xie C, Zhao Y, Mao X, Gao H, Ma J (2022) Effects of African BaP emission from wildfire biomass burning on regional and global environment and human health. Environ Int 162:107162. https://doi.org/10.1016/j.envint.2022.107162

Wu K, Meng Y, Gong Y, Zhang X, Wu L, Ding X, Chen X (2022) Surveillance of long-term environmental elements and PM2.5 health risk assessment in Yangtze River Delta, China, from 2016 to 2020. Environ Sci Pollut Res Int. https://doi.org/10.1007/s11356-022-21404-6

Yan D, Wu S, Zhou S, Tong G, Li F, Wang Y, Li B (2019) Characteristics, sources and health risk assessment of airborne particulate PAHs in Chinese cities: a review. Environ Pollut 248:804–814. https://doi.org/10.1016/j.envpol.2019.02.068

Yancheshmeh RA, Bakhtiari AR, Mortazavi S, Savabieasfahani M (2014) Sediment PAH: contrasting levels in the Caspian Sea and Anzali Wetland. Mar Pollut Bull 84(1–2):391–400. https://doi.org/10.1016/j.marpolbul.2014.05.001

Yang L, Suzuki G, Zhang L, Zhou Q, Zhang X, Xing W, Shima M, Yoda Y, Nakatsubo R, Hiraki T, Sun B, Fu W, Qi H, Hayakawa K, Toriba A, Tang N (2019) The characteristics of polycyclic aromatic hydrocarbons in different emission source areas in Shenyang, China. Int J Environ Res Public Health 16(16):2817. https://doi.org/10.3390/ijerph16162817

Yao Y, Wu Y, Zhu P, Meng Y, Zhu H (2021) Evaluation of uncertainty in determination of polycyclic aromatic hydrocarbons in atmospheric PM2.5 by high performance liquid chromatography. Chem Anal Meterage. https://doi.org/10.3969/j.issn.1008-6145.2021.05.017

Yazdani M (2020) Comparative toxicity of selected PAHs in rainbow trout hepatocytes: genotoxicity, oxidative stress and cytotoxicity. Drug Chem Toxicol 43(1):71–78. https://doi.org/10.1080/01480545.2018.1497054

Yu X, Li C, Chen H, Ji Z (2020) Evaluate air pollution by Promethee ranking in Yangtze River Delta of China. Int J Environ Res Public Health 17(2):587. https://doi.org/10.3390/ijerph17020587

Yu Z, Wang H, Zhang X, Gong S, Liu Z, Zhao N, Zhang C, Xie X, Wang K, Liu Z, Wang JS, Zhao X, Zhou J (2022) Long-term environmental surveillance of PM2.5-bound polycyclic aromatic hydrocarbons in Jinan, China (2014–2020): Health risk assessment. J Hazard Mater 425:127766. https://doi.org/10.1016/j.jhazmat.2021.127766

Zaragoza-Ojeda M, Torres-Flores U, Rodríguez-Leviz A, Arenas-Huertero F (2022) Benzo[ghi]perylene induces cellular dormancy signaling and endoplasmic reticulum stress in NL-20 human bronchial epithelial cells. Toxicol Appl Pharmacol 439:115925. https://doi.org/10.1016/j.taap.2022.115925

Zhang X, Lu W, Xu L, Wu W, Sun B, Fan W, Zheng H, Huang J (2022) Environmental risk assessment of polycyclic aromatic hydrocarbons in farmland soils near highways: a case study of Guangzhou, China. Int J Environ Res Public Health 19(16):10265. https://doi.org/10.3390/ijerph191610265

Zhang X, Leng S, Qiu M, Ding Y, Zhao L, Ma N, Sun Y, Zheng Z, Wang S, Li Y, Guo X (2023) Chemical fingerprints and implicated cancer risks of Polycyclic aromatic hydrocarbons (PAHs) from fine particulate matter deposited in human lungs. Environ Int 173:107845. https://doi.org/10.1016/j.envint.2023.107845

Zhao W, Liu X, Deng Q, Li D, Xu J, Li M, Cui Y (2020) Spatial association of urbanization in the Yangtze River Delta, China. Int J Environ Res Public Health 17(19):7276. https://doi.org/10.3390/ijerph17197276

Zhu J, Zhang X, Zhang X, Dong M, Wu J, Dong Y, Chen R, Ding X, Huang C, Zhang Q, Zhou W (2017) The burden of ambient air pollution on years of life lost in Wuxi, China, 2012–2015: a time-series study using a distributed lag non-linear model. Environ Pollut 224:689–697. https://doi.org/10.1016/j.envpol.2017.02.053

Zonkpoedjre S, Zonkpoedjre S, Ezeorah C, Nwani CD (2022) Sources, pollution, and ecological risk assessment of polycyclic aromatic hydrocarbons (PAHs) in Porto-Novo Lagoon, Benin Republic. Environ Geochem Health. https://doi.org/10.1007/s10653-022-01250-8